Cross-Sectional Warping in Sheet Metal Forming Simulations

Tobias Willmann[1], Alexander Wessel[2], Thorsten Beier[3], Alexander Butz[2], Manfred Bischoff[1]

[1]Institute for Structural Mechanics, University of Stuttgart
Pfaffenwaldring 7, 70550 Stuttgart, Germany
{willmann;bischoff}@ibb.uni-stuttgart.de

[2]Fraunhofer Institute for Mechanics of Materials IWM
Woehlerstrasse 11, 79108 Freiburg, Germany
{alexander.wessel;alexander.butz}@iwm.fraunhofer.de

[3]thyssenkrupp Steel Europe AG
Eberhardstrasse 12, 44145 Dortmund, Germany
thorsten.beier@steeleurope.com

Abstract

For most sheet metal forming simulations, shell elements that consider a reduced stress state, in particular, assuming a zero transverse normal stress σ_{33} and neglecting the shear stress components σ_{13} and σ_{23} in the yield function, are used. Moreover, certain kinematic assumptions, like cross-sectional material fibers being assumed to remain straight during deformation, are typically applied. However, for some applications, like bending with small radii and thick sheets, this approach is not a workable solution to obtain accurate and reliable results, since the prerequisites that justify the aforementioned kinematic assumptions are not met anymore.

In this contribution, a 3d-shell element is presented that allows for cross-sectional warping. For the evaluation, numerical results of a metal stripe drawn through a draw bead are compared against experimental data. The results demonstrate that the 3d-shell element is able to represent warping of cross-sectional material fibers during deformation. In addition, further numerical tests conducted with this element are shown.

1 Introduction

The results of numerical simulations of some applications, like bending with small radii and thick sheets, are not sufficiently accurate when performed with standard shell elements, since standard shell elements are based on certain assumptions that are not met in these cases. Besides a more precise material description, one of our research goals within the research project "Verbesserte Blechumformsimulation durch 3D-Werkstoffmodelle und erweiterte Schalenformulierungen" [1] is to develop a 3d-shell element that allows for cross-sectional warping and therefore captures the deformation of the sheet metal more precisely. This contribution shows parts of the results obtained from this project. A detailed presentation of the project results can be found in the project report [2]. This paper presents excerpts from the report and is therefore closely related to [2].

This paper is structured as follows. First, the theory of the 3d-shell element used in the calculations is explained, see Section 2. In Section 3, the experimental setup of the draw bead tests as well as the results are presented and compared to numerical simulations. Section 4 shows further numerical tests conducted with this element.

2 3d-shell element

In contrast to shell elements currently available in LS-DYNA, the 3d-shell element used for the simulations in this paper allows for cross-sectional warping and a strain field up to third order with respect to the thickness coordinate. In the following, this element is called 3DBM-13.

The element is formulated based on the velocity strains $\mathbf{d}$, corresponding to the symmetric part of the velocity gradient $\mathbf{l}$, as the strain measure. This requires the description of the geometry as well as the velocity field. For 3DBM-13 these are

$$\mathbf{x}\,(\theta^1,\theta^2,\theta^3) = \bar{\mathbf{x}}\,(\theta^1,\theta^2) + \theta^3\mathbf{n}(\theta^1,\theta^2) + L_2(\theta^3)\mathbf{p}(\theta^1,\theta^2) + L_3(\theta^3)\mathbf{q}(\theta^1,\theta^2),$$
$$\mathbf{v}\,(\theta^1,\theta^2,\theta^3) = \bar{\mathbf{v}}\,(\theta^1,\theta^2) + \theta^3\dot{\mathbf{n}}(\theta^1,\theta^2) + L_2(\theta^3)\dot{\mathbf{p}}(\theta^1,\theta^2) + L_3(\theta^3)\dot{\mathbf{q}}(\theta^1,\theta^2).$$

The symbols used in the previous equations are:

- $\bar{\mathbf{x}}\,(\theta^1,\theta^2)$: midsurface position in the current configuration
- $\bar{\mathbf{v}}\,(\theta^1,\theta^2)$: midsurface velocity
- $\mathbf{n}(\theta^1,\theta^2)$, $\mathbf{p}(\theta^1,\theta^2)$ und $\mathbf{q}(\theta^1,\theta^2)$: first, second and third order director
- $\dot{\mathbf{n}}(\theta^1,\theta^2)$, $\dot{\mathbf{p}}(\theta^1,\theta^2)$ und $\dot{\mathbf{q}}(\theta^1,\theta^2)$: rate of the first, second and third order director
- $L_2(\theta^3) = \frac{1}{2}(3\,(\theta^3)^2 - 1)$: quadratic Legendre polynomial
- $L_3(\theta^3) = \frac{1}{2}(5\,(\theta^3)^3 - 3\,\theta^3)$: cubic Legendre polynomial

The midsurface velocity $\bar{\mathbf{v}}$ as well as the rates of the directors $\dot{\mathbf{n}}$, $\dot{\mathbf{p}}$ und $\dot{\mathbf{q}}$ are each vectors with three degrees of freedom, resulting in twelve degrees of freedom for 3DBM-13. The 13th degree of freedom is a parameter, which adds a cubic strain field in thickness direction.

Figure 1 visualizes the various parts of the deformation. The element is able to rotate its directors with respect to the midsurface (left). Furthermore, cross-sectional fibers can deform with a quadratic and cubic shape (center and right).
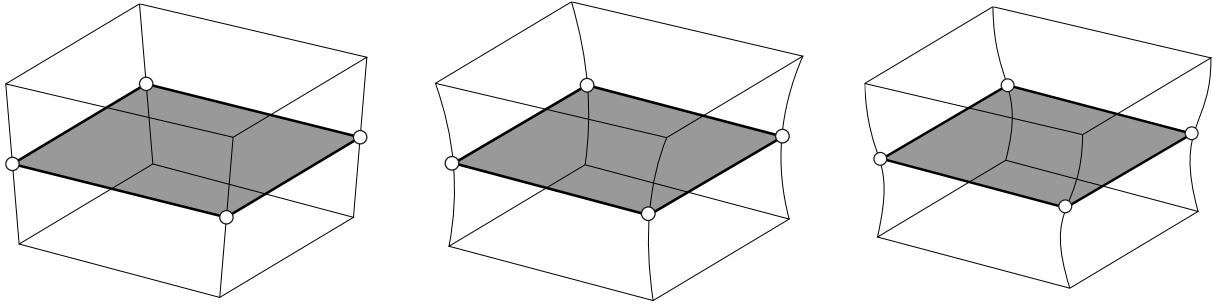
Fig.1: Visualization of the deformation modes of 3DBM-13 including linear (left), quadratic (center) and cubic (right) shapes of cross-sectional fibers.

The velocity gradient, which can be derived from the velocity and displacement field given above, is a rational function of the thickness coordinate θ^3. Assuming appropriate differentiability, which is given for a regular element form, the velocity gradient can be written as a Taylor series with the evaluation point $\theta^3 = 0$:

$$\mathbf{l} = \sum_{k=0}^{\infty} \frac{\mathbf{l}^{(k)}(\theta^3 = 0)}{k!}\,\theta^3.$$

For 3DBM-13, twelve degrees per node of freedom are considered to take constant, linear, quadratic and cubic contributions to the cross-sectional deformation into account:

$$\mathbf{l}^{\text{3DBM}-13} = \sum_{k=0}^{3} \frac{\mathbf{l}^{(k)}(\theta^3 = 0)}{k!}\,\theta^3.$$

Furthermore, it is possible to sort the strain displacement operator B by the power of θ^3. Hence, it can be written as

$$B_{ijp} = \sum_{c=0}^{n} B_{ijp}^c \cdot (\theta^3)^c.$$

This is advantageous in terms of computation time, since the coefficients B_{ijp}^c depend only on θ^1 and θ^2 and are thus computed only as many times as there are integration points in the shell plane. For the integration points in the thickness direction, the strain displacement operator can then be obtained directly from the linear combination above.

To avoid transverse shear locking, the assumed natural strain method is used. The corresponding transverse shear velocity strains are evaluated at the collocation points and interpolated in the element. Details on this method can be found in [3]. In addition to transverse shear locking, locking effects in the shell plane must also be avoided. These two effects, in-plane shear locking and in-plane volumetric locking, can also be avoided with established methods, for example the Enhanced Assumed Strain Method (EAS) [6]. Methods against in-plane locking are not implemented for the simulations shown in the following sections, since these effects are of minor importance for the examples investigated.

3 Evaluation of shell element using draw bead experiments

For the evaluation of the shell element presented in the previous section, numerical results of a metal stripe drawn through a draw bead are compared against experimental data. We first explain the experimental procedure, followed by a comparison of experimental and numerical results.

3.1 Experimental procedure

To perform draw bead experiments, specimens are manufactured in a two-step process. First, sheets made of DX56D deep drawing steel are cut into stripes with a length of 430 mm and a width of 29.5 mm using water jet cutting. Second, to investigate the cross-sectional curvature during the experiment, holes are drilled through the 1.5 mm thick specimens. To minimize the effect of the holes on the deformation behavior, the diameter of the holes is set to a relatively small value of 1.0 mm.

The draw bead experiments are conducted at thyssenkrupp Steel Europe AG using a uniaxial testing machine equipped with a draw bead as shown in Figure 2. The stripes are clamped in the lower tool, which is then moved downwards with the constant velocity of 10 mm/s. Two different types of draw bead experiments are carried out:

- **Stopped experiments:** these experiments are performed until the holes reached the draw bead and then terminated, see Figure 3 (left). The aim of these experiments is to provide information on the change of the cross-sectional curvature while the metal stripe is passing the draw bead.

- **Unstopped experiments:** In addition to the stopped experiments, unstopped tests are performed, i.e. the metal stripe is drawn through the draw bead completely. Hence, the results of this experiment provide additional information regarding the cross-sectional curvature in thickness direction after passing the draw bead.

After performing the draw bead experiments, the holes of the metal stripes are examined metallographically to visualize the warping of cross-sectional fibers, see Figure 3 (right). To this end, light microscopic pictures of the holes in the longitudinal cross-section are taken using a Leica M80 microscope.
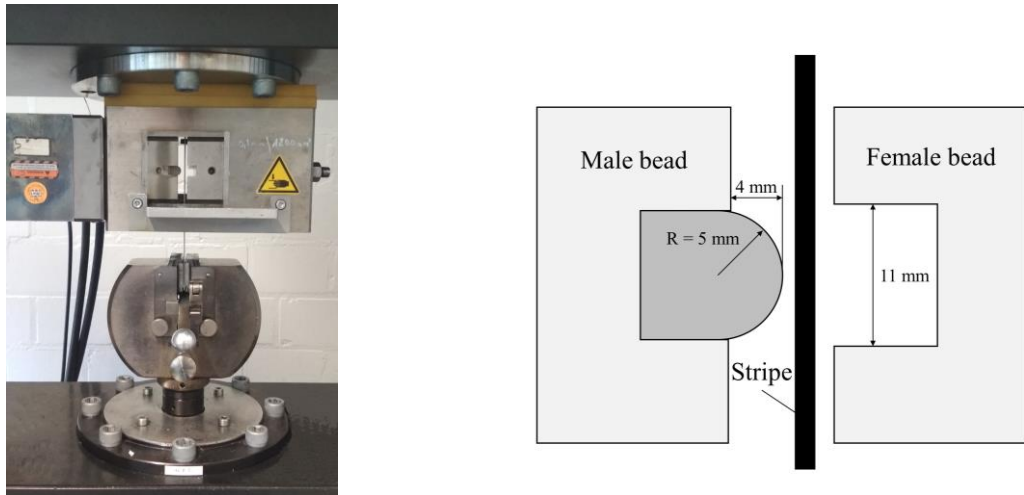
Fig.2: Setup of the draw bead experiment: uniaxial testing machine equipped with a draw bead (left) and schematic representation of the draw bead (right).
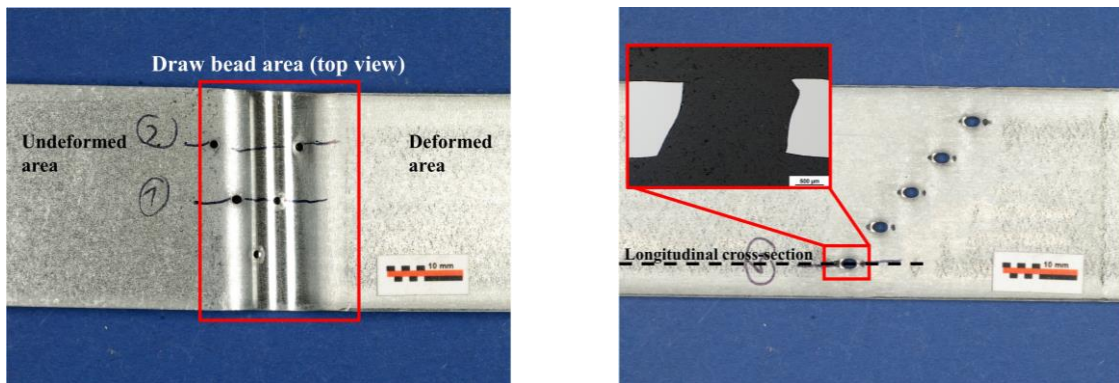
Fig.3: Specimens of the stopped (left) and unstopped draw bead experiments including an exemplary microscopically analysis (right).

3.2 Comparison of simulation results and experimental data

Results of the stopped and unstopped experiments are illustrated in Figure 4 for different stages of deformation in the draw bead experiment. It can be seen that the sheet had initially straight cross-sectional fibers, which got warped while passing the draw bead. After the stripe passed the draw bead, the cross-sectional fibers exhibit a strong warping.
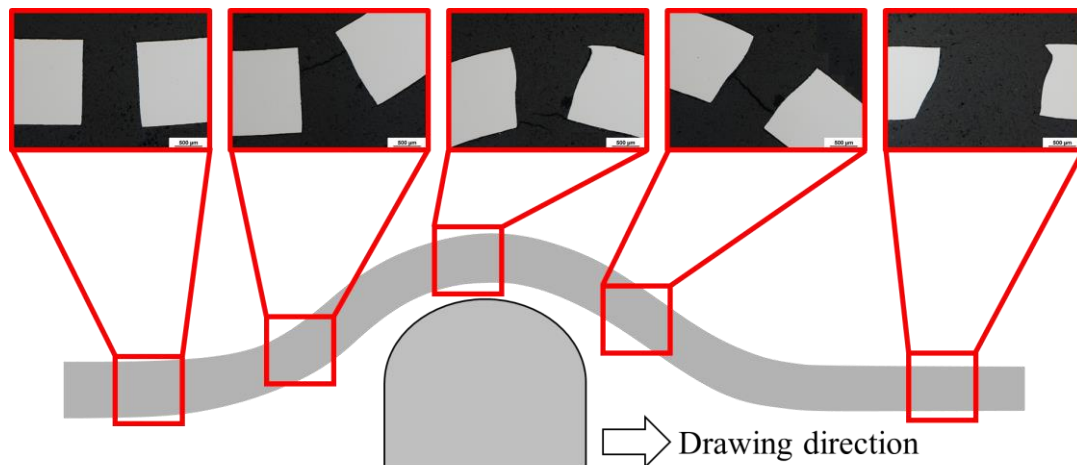
Fig.4: Experimental results: cross-sectional warping during the draw bead experiment.

Figure 5 compares the cross-sectional warping determined in the experiments with the warping visible in the simulation with solid elements and the 3DBM-13 shell elements. Since 3DBM-13 is represented by its midsurface, i.e. it is a four-node shell element, the deformation in thickness direction is not visible in standard post-processing tools. In order to make the cross-sectional deformation of 3DBM-13 visible, a solid-like visualization is implemented, see Figure 5 (center). Standard shell elements are not considered as this type of element is not able to take cross-sectional warping into account. Qualitatively, both the solids and the 3DBM-13 shells show a similar cross-sectional warping compared to the experimental results. Close to the bottom side of the sheet, the cross-section fiber forms a 90° angle with the lower edge of the sheet in the simulation with both solids and 3DBM-13 shells. However, this is not the case in the experiment. Close to the top side of the sheet, the warping representation of 3DBM-13 is slightly underestimated whereas the warping representation of the solid simulation slightly overestimates the deformation obtained from experiments. Nevertheless, further studies with finer discretization in the sheet plane are needed to draw final conclusions about the approximation quality.

Solids   3DBM-13   Experiment
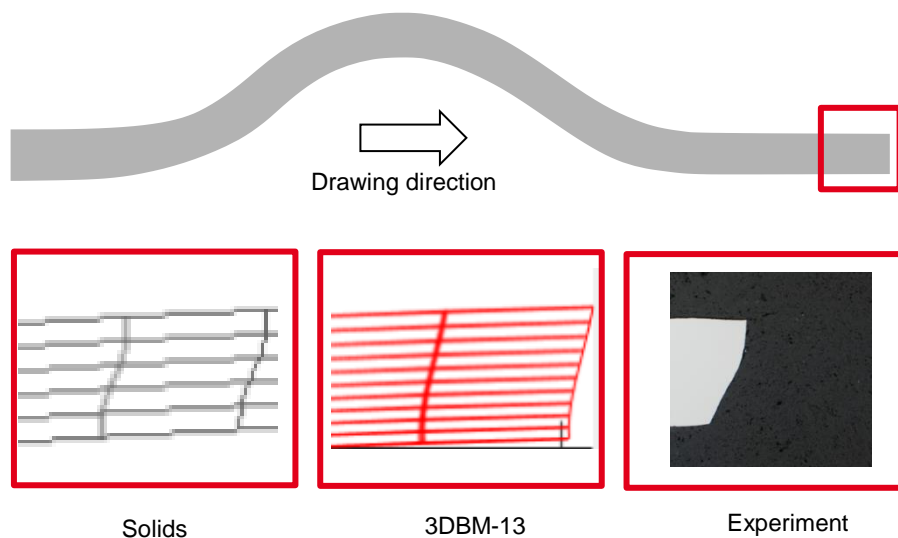
Fig.5:   *Comparison of cross-sectional warping over the sheet thickness: simulations with solids (left), 3DBM-13 shell elements (center) as well as experimental results (right).*

4 Further numerical tests

4.1 Contact representation

An important property of finite elements for sheet metal forming simulations is the correct representation of contact. In numerous situations, friction between tools and the sheet metal induces deformations and thus stresses in the sheet metal. To demonstrate the advanced capabilities of the developed element, a single-element contact test is performed. In order to facilitate comparison of the results with an analytical solution, the test is performed with an elastic material law. The definition of this test is shown in Figure 6 (left). The figure shows a side view of a shell element, the dashed lines indicate the shell thickness, the solid line symbolizes the shell midsurface. To generate contact normal stresses, the nodes of the element are first moved in the negative z-direction by displacement boundary conditions. Subsequently, the nodes are moved in the positive x-direction, also by displacement boundary conditions, as indicated by the displacement u in Figure 6 (left). As the element slides along the plane, shear stresses are generated. It can be expected that the shear stresses at the contact surface are given by

$$\tau_{xz} = \mu|\sigma_z|.$$

At the same time, it is to be expected that the shear stress is zero at the upper side of the element, since the upper side is a free surface without any external stresses applied. A simulation of the described test with the shell element of Belytschko-Tsay [4], implemented in LS-DYNA as shell element 2, results in zero shear stress over the entire plate thickness, see Figure 6 (right). 3DBM-13

exactly fulfills the expected conditions with respect to the stress values on the top and bottom side and shows a linear progression in between. This suggests a significantly improved representation of situations in which shear stresses induced from contact play an important role, such as the passage of a sheet through a drawing bead.
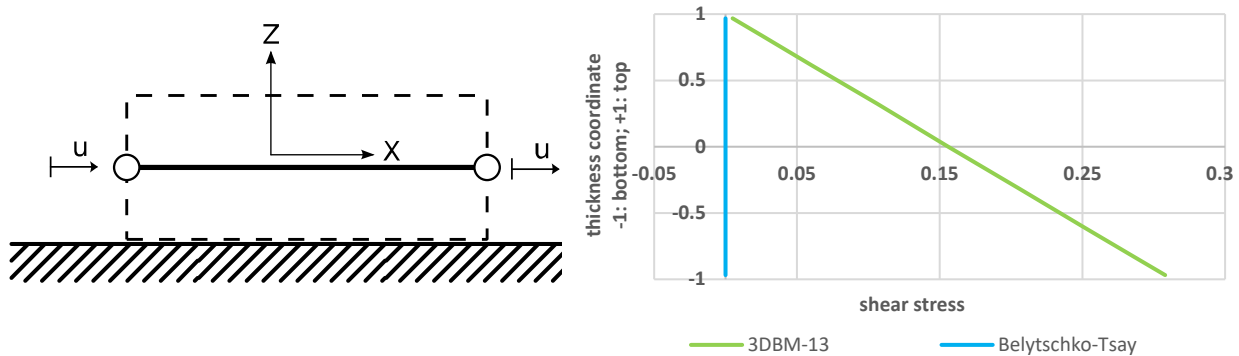
Fig.6:   One element contact and shear test; setup (left) and shear stress distribution (right).

4.2   Bending of a thick sheet

An important goal of our work is to improve the representation of situations in which the assumptions of standard shell elements are no longer valid. This is also the case, for example, in situations where a sheet is bent around a radius that is small in relation to the sheet thickness. Such a numerical experiment is shown in Figure 7. The left image shows the simulation with continuum elements, which will be used as a reference in the following. The picture on the right-hand side of Figure 7 shows the simulation with shell elements. An initially flat sheet metal strip is bent in a three-point bending test as shown. The two outer rollers are fixed and the middle one is subjected to an inhomogeneous displacement boundary condition, causing the sheet to bend. The sheet thickness is 1.5 mm, radius of punch and supports are 1 mm each. The material data for these models is taken from a material characterization of DX56D, see [2]. For the reference solution, 16 elements are used across the sheet thickness, and the element edge length in the sheet plane is 0.125 mm. For the simulation with shell elements, an element edge length of 0.125 mm is chosen in the areas of large deformation, and 0.25 mm in the other areas.
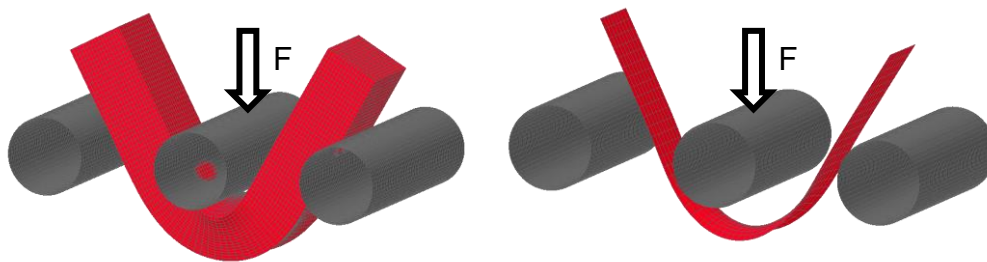
Fig.7:   Three-point bending test conducted with shell and solid elements.

Figure 8 plots the deformed geometry with the reference solution with solid elements on the left, the solution with 3DBM-13 in the center and for comparison the solution with a shell element based on the assumption of cross-sectional fibers remaining straight on the right-hand side. A solid-like visualization is used for shell elements to visualize the solution in thickness direction. In the results a similar cross-sectional curvature is visible in both the solid solution and the solution using 3DBM-13. In the solution with straight cross-sectional fibers, no warping can occur per definition, resulting in a noticeably worse geometry approximation. The three bottom figures show the same deformation state in a frontal view. To illustrate the warping of the cross-section, straight dashed lines are drawn for comparison. Again, 3DBM-13 shows a qualitatively similar cross-sectional warping as the reference solution with solids. For standard shell elements, according to the assumption, the cross-sectional fibers remain straight.

Nonlinear deformation in thickness direction
Cross-sectional fibers do not remain straight

Cross-sectional fibers remain straight (standard shell assumption)
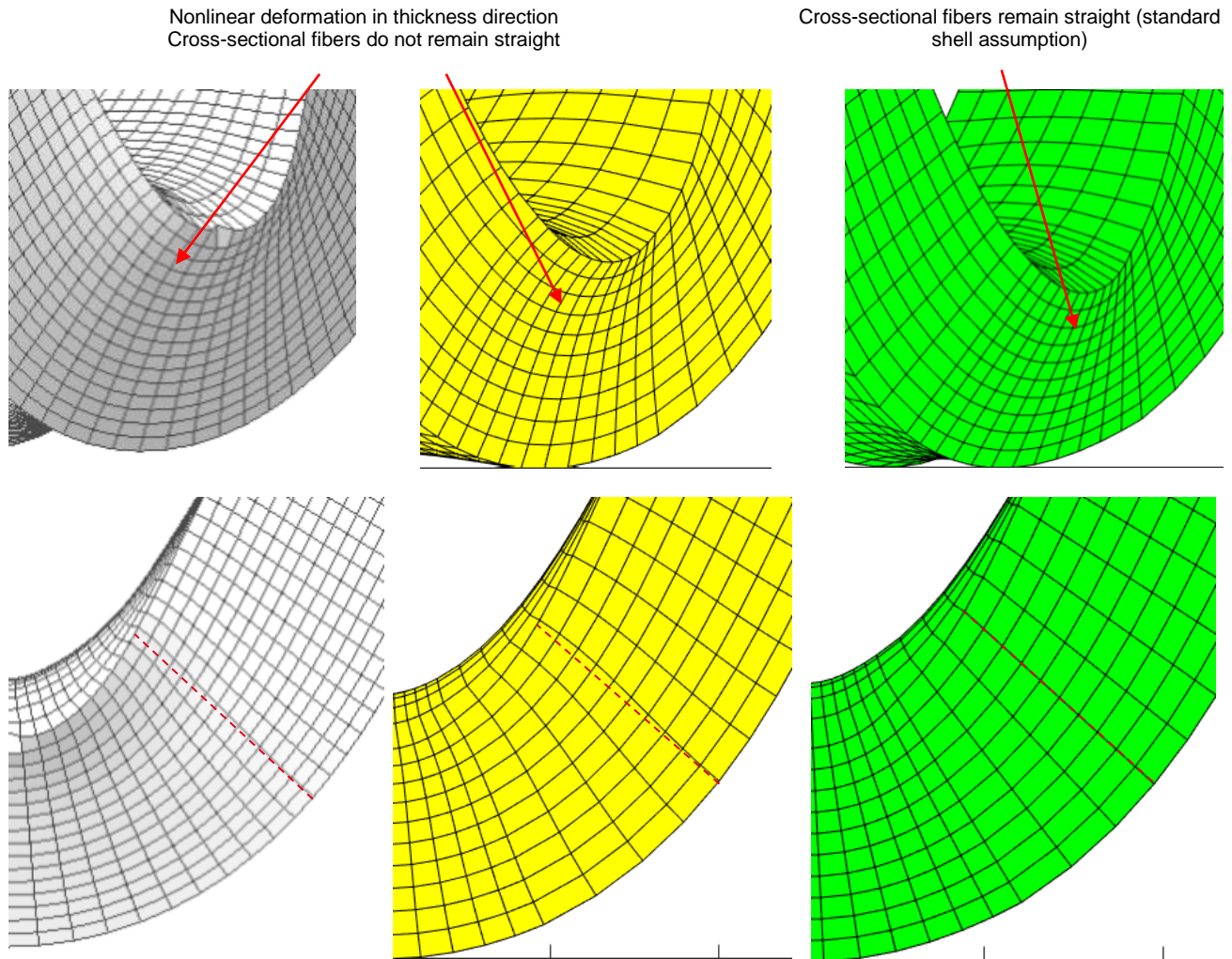
Fig.8: *Deformed cross-sectional fibers in the 3-point bending test with a thick sheet for solids (left), 3DBM-13 (center) and shell elements based on straight fibers (right).*

5 Summary and outlook

A 3d-shell element with the capability to represent warped cross-sectional fibers is presented. Results of various numerical tests indicate that this element is able to represent the behavior in critical sheet metal forming simulations qualitatively correct.

Further aspects need to be addressed in order to make the element usable in industrial applications. The performance of the element needs to be improved by using reduced integration and mass scaling for the higher order degrees of freedom, among other things. Furthermore, detailed quantitative investigations are necessary to evaluate the benefits in practical applications. These aspects are currently being worked on in a follow-up project [5].

6 Acknowledgement

7 Literature

[1] Research project "Verbesserte Blechumformsimulation durch 3D-Werkstoffmodelle und erweiterte Schalenformulierungen", EFB 09/117, AiF 19707N

[2] Butz, A., Wessel, A., Bischoff, M., Willmann, T.: "Verbesserte Blechumformsimulation durch 3D-Werkstoffmodelle und erweiterte Schalenformulierungen", 2020, ISBN: 978-3-86776-588-6

[3] Bathe, K.J., Dvorkin, E.N.: "A formulation of general shell elements – The use of mixed interpolation of tensorial component", International Journal for Numerical Methods in Engineering 22, 1986

[4] Belytschko, T., Lin, J., Tsay, C.: "Explicit algorithms for the nonlinear dynamics of shells", Computer Methods in Applied Mechanics and Engineering 42, 1984, p. 225-251

[5] Research project "Verbesserte Blechumformsimulation durch 3D-Werkstoffmodelle und erweiterte Schalenformulierungen – Teil 2", EFB 06/219, AiF 21466N, https://www.efb.de/21466n.html

[6] Simo, J., Rifai, M.; "A class of mixed assumed strain methods and the method of incompatible modes", International Journal for Numerical Methods in Engineering 29.9, 1990, p. 1595-1638